Explicit Dosimetry for Photodynamic Therapy; Singlet Oxygen Modeling based on Finite-Element Method

Ken Kang-Hsin Wang[*,1] and Timothy C. Zhu[1]
[1]Department of Radiation Oncology, School of Medicine, University of Pennsylvania, Philadelphia, PA 19104
*Corresponding author: Radiation Oncology, University of Pennsylvania, 3400 Spruce Street/2 Donner Bldg, Philadelphia, PA 19104, wangken@xrt.upenn.edu

Abstract: Singlet oxygen ($^1O_2$) is the major cytotoxic agent during type-II photodynamic therapy (PDT). The production of $^1O_2$ involves the complex reactions among cancer agent, oxygen molecule, and treatment laser light. The reacted $^1O_2$ concentration, $[^1O_2]_{rx}$, can be expressed in a form related to time integration of the product of $^1O_2$ quantum yield and the PDT dose rate. The light propagation in tumor tissue is described by the diffusion equation. Incorporating light transport phenomena, oxygen supply and consumption mechanism, and photochemically $^1O_2$ production procedures, the spatially and temporally-resolved $[^1O_2]_{rx}$ can be numerically calculated. A flat region close to the light source location is observed, and this suggests a possible correlation between $[^1O_2]_{rx}$ and tumor necrosis boundary. In this work, an optimization routine is developed to fit the $[^1O_2]_{rx}$ profile to the simulated necrosis distance. If modeling parameters can be determined precisely through the fitting algorithm, we expect that this $^1O_2$ model can be used as an explicit dosimetry to optimize the treatment efficacy.

Keywords: Photodynamic therapy, Singlet oxygen, Optimization routine, necrosis, Explicit dosimetry

1. Introduction

Singlet oxygen ($^1O_2$) is the major cytotoxic agent during type II photodynamic therapy (PDT), and the reaction between $^1O_2$ and tumor cells defines the most fundamental treatment efficacy [1]. It has been a long-term issue to correlate/quantify the amount of $^1O_2$ with tumor death in PDT field. The production of $^1O_2$ involves the complex reactions among cancer agent (photosensitizer), oxygen molecule, and treatment laser light. From a complete set of the macroscopic kinetic equations which describe the photochemical processes of PDT, we can express the reacted $^1O_2$ concentration, $[^1O_2]_{rx}$, in a form related to time integration of the product of $^1O_2$ quantum yield and the PDT dose rate. The light propagation in tumor tissue is described by the diffusion equation. A term describing the physiological oxygen supply phenomena is introduced in the kinetic equations set. Incorporating light transport phenomena in turbid medium, oxygen supply and consumption mechanism, and photochemically $^1O_2$ production procedures, the spatially and temporally-resolved $[^1O_2]_{rx}$ can be numerically calculated.

Interestingly, we observe a plateau region of $[^1O_2]_{rx}$ profiles close to the light source location [2], and this suggests a possible correlation between $[^1O_2]_{rx}$ and tumor necrosis boundary. There are a few parameters describing the photochemical process of the PDT, which needs to be determined precisely for a specific drug. To obtain the most accurate modeling parameters, we propose to measure the PDT-induced necrosis range, and fit the calculated $[^1O_2]_{rx}$ profile to the necrosis regime. In this case, these modeling parameters are extracted from an *in vivo* environment closely related to a clinical setup, and our singlet oxygen model is expected to be used as an explicit dosimetry.

In this work, an optimization routine is developed. To examine the fitting ability of our algorithm, we prepare a mathematical phantom and simulate the $[^1O_2]_{rx}$ profiles corresponding to different treatment conditions. Our algorithm can accurately recover the modeling parameters within a reasonable computational time frame. To further fitting the necrosis distance, a series of interstitial PDT treatment *in vivo* experiments have been conducted, and the measurable necrosis distance are observed for different treatment conditions. The procedures of fitting measured necrosis distance are also discussed in this wok.

2. Method

2.1 Singlet oxygen model

The following are the governing equations of our macroscopic singlet oxygen model.

$$(\mu_a + \varepsilon \cdot u_2)u_1 - \nabla \cdot \left(\frac{1}{3\mu_s'}\nabla u_1\right) = S \quad (1)$$

$$\frac{du_2}{dt} + \left(S_\Delta \gamma\eta \frac{\kappa}{1+\alpha}\frac{u_1 u_2 u_3}{u_3+\beta}\right)u_2 = 0 \quad (2)$$

$$\frac{du_3}{dt} + \left(S_\Delta \gamma\eta \frac{\alpha}{1+\alpha}\frac{u_1 u_2}{u_3+\beta}\right)u_3 - g\left(1 - \frac{u_3}{u_3(t=0)}\right) = 0 \quad (3)$$

$$\frac{du_4}{dt} - \left(fS_\Delta \gamma\eta \frac{\alpha}{1+\alpha}\frac{u_1 u_2 u_3}{u_3+\beta}\right) = 0 \quad (4)$$

For the sake of convenience, we use u_1, u_2, u_3, and u_4 to name light fluence rate ϕ, the concentrations of sensitizer [S_0], oxygen [$^3O_2$], and reacted singlet oxygen $[^1O_2]_{rx}$. $[^1O_2]_{rx}$ is the $[^1O_2]$ reacting with cell targets, which is the dosimetry quantity fundamentally determining the treatment efficacy. In the cases we considered here, but not limited, μ_a, μ_s', ε, and S are the absorption, reduced scattering coefficients at treatment wavelength (630 nm here), extinction coefficient for photosensitizer at the treatment wavelength, and source strength in mW/cm for a linear source. α, β, γ, κ, η and S_Δ are the photophysical parameters for photosensitizer. The detail of the origin and definition can be found in [3]. g is the maximum oxygen supply rate, and f is the fraction of $[^1O_2]_{rx}$ efficiently inducing cell death. In this work, we set f equal to one. The complex photochemical parameters can be further lumped into 3 independent parameters, where $\xi = S_\Delta \gamma\eta\alpha/(1+\alpha)$, $\rho = \kappa/\alpha$, and β. In the case we considered here, Photofrin-PDT at 630 nm, the sensitizer extinction coefficient ε is 0.0035 (cm^{-1} uM^{-1}) [4] and the initial *in vivo* Photofrin concentration is around 7 μM 24 hr after 5 mg/kg *i.v.* injection [5]. Therefore, the absorption coefficient for Photofrin is 0.025 (cm^{-1}), which is 28 folder lower than the absorption coefficient of tumor tissue such as 0.71 (cm^{-1}) measured interstitially (data not shown). We therefore can treat Eq. (1) as a steady state equation, solving it independently from the other three time dependent Eqs. (2-4). The final modeling equations are listed here as

$$\mu_a u_1 - \nabla \cdot \left(\frac{1}{3\mu_s'}\nabla u_1\right) = S \quad (5)$$

$$\frac{du_2}{dt} + \left(\xi\rho \frac{u_1 u_2 u_3}{u_3+\beta}\right)u_2 = 0 \quad (6)$$

$$\frac{du_3}{dt} + \left(\xi \frac{u_1 u_2}{u_3+\beta}\right)u_3 - g\left(1 - \frac{u_3}{u_3(t=0)}\right) = 0 \quad (7)$$

$$\frac{du_4}{dt} - \left(\xi \frac{u_1 u_2 u_3}{u_3+\beta}\right) = 0 \quad (8)$$

Therefore, we have 4 independent parameters g, ξ, ρ, and β, which needs to be determined precisely.

Because the PDT clinical trial conducted in University of Pennsylvania focuses on interstitial linear source treatment within prostate, we can use cylindrical geometry describing the space in which light propagates (Eq. (5)), and solve the PDT Eqs. (6-8) along the radial axis with respect to the linear source.

2.2 Use of COMSOL Multiphysics

As describing above, modeling $[^1O_2]_{rx}$ production is not a trivial problem, which involves complicated process and reactions among sensitizer, light, and oxygen. Moreover, fitting the measured necrosis distance requires fast calculation technique being able to quickly compute the results in different treatment conditions. Finite element method based COMSOL Multiphysics combined with MATLAB is a great candidate for this purpose.

Figure 1 shows the flow chart of our fitting algorithm routine. After we input the parameters and 1D necrosis profile, we can decide the fitting scheme, fixing g, fixing ξ, ρ, and β, or relaxing these 4 parameters. The main program *LSmodel.m* coded in MATLAB environment will execute calculation procedure by calling COMSOL model. We first solve steady state light diffusion equation (Eq. (5)) for a linear source in a 3D cylindrical geometry, built in a COMSOL environment. Due to the symmetrical feature of the cylinder, we are only interested in the light distribution along 1D radial axis. This 1D light distribution profile will be passed to next step, the calculation of PDT kinetics equation (Eqs. (6-8)). Again, due to the cylindrically-symmetrical feature, we can consider the $[^1O_2]_{rx}$ production in 1D radial axis. The algorithm then generates the $[^1O_2]_{rx}$ profiles for different treatment conditions, and fits the necrosis distance. The differential evolution

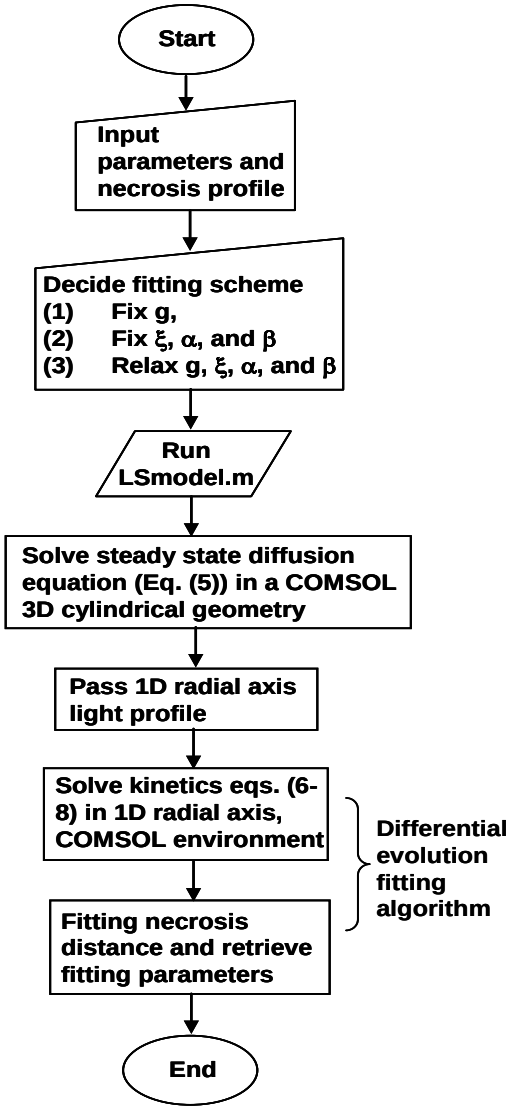

Figure 1: Flow chart of COMSOL-MATLAB fitting routine. Differential evolution algorithm is chosen as the core fitting technique.

algorithm developed by Storn *et al.*[6] and modified by us are used as the optimization routine. It is an efficient direct-search algorithm for nonlinear problem. Our goal is to minimize the maximum deviation MAX(|fit/data - 1|) between data and fit.

Table 1 lists the boundary, initial conditions, and other necessary parameters used in this model [2]. Here, the literature values of g, ξ, ρ, and β are listed here [2]. The value of the initial conditions of u_2 and u_3 are extracted from *in vivo* experiment. The values of μ_a and μ_s' are determined by interstitial point source technique [7] within RIF mice tumor.

Table 1. Boundary, initial conditions, and parameters for singlet oxygen model

Boundary conditions	$u_{i=2,3,4}$	$\nabla u_i = 0$
Initial conditions	u_2	7 μM
	u_3	83 μM
	u_4	0
Light associated parameters	u_a	0.71 (cm^{-1})
	u_s'	9.14 (cm^{-1})
Physiological parameter	g	0.7
Photochemical Parameter (for Photofrin)	ξ	3.7 x 10^{-3} (cm^2/mWs)
	ρ	7.6 x 10^{-5} (1/μM)
	β	11.9 μM

2.3 Interstitial PDT treatment

To rigorously quantify $[^1O_2]_{rx}$ in an *in-vivo* environment, a series of preclinical experiments are proposed to generate the PDT-induced necrosis within RIF tumor model grown on C3H mice shoulder.

In preliminary studies, mice bearing subcutaneous RIF tumors were treated with interstitial Photofrin (5 mg/kg, 24 h) PDT using a 1 cm linear diffusing fiber and illumination with 38, 75, and 150 mW/cm and 25 to 100 J/cm. The wide range of light delivery conditions was used to quantify the threshold light dose necessary to induce a measurable radius of necrosis and therefore robustly determine the modeling parameters. For assessment of the radius of necrosis, treated tumors were excised from euthanized animals at 24 h after PDT and fixed in formalin. Hematoxylin and eosin (H&E) staining was performed at the Pathology Core Labs, Children's Hospital of Philadelphia.

3. Results and Discussions

3.1 Numerical results simulating *in vivo* Photofrin-PDT treatment

Figure 2 shows our modeling calculation using the parameters listed in Table 1. The fluence rate and fluence are the treatment parameters. Fig. 2 (A), (B), and (C) are the sensitizer, oxygen, and reacted singlet oxygen

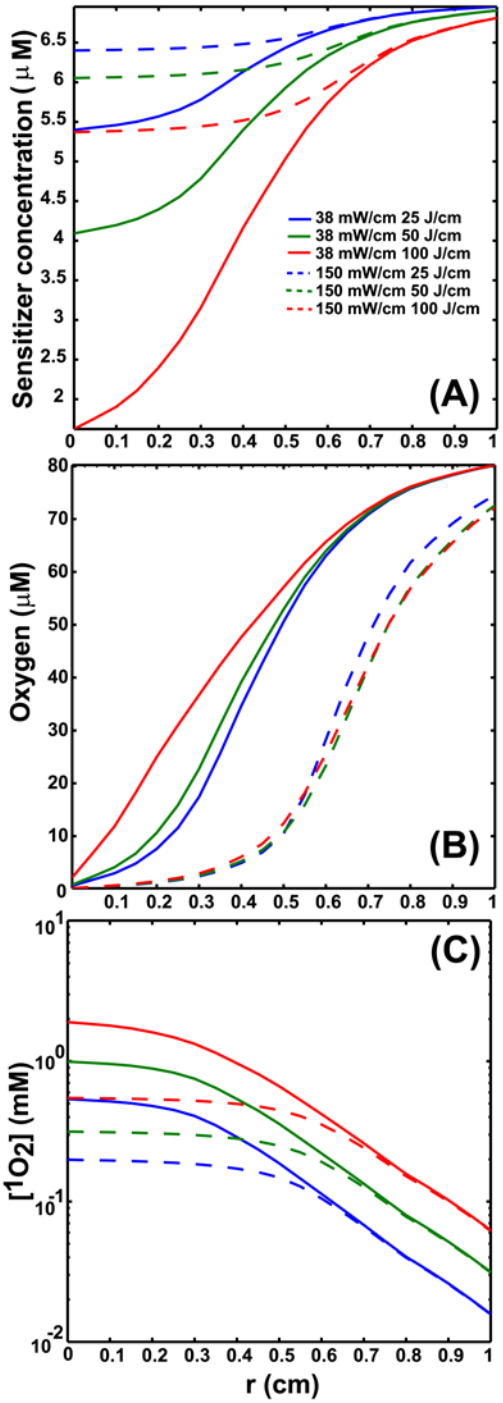

Figure 2: Sensitizer (A), oxygen (B), and reacted singlet oxygen (C) *vs.* radial distance with respect to a linear source for 38 and 150 mW/cm for 25, 50, and 100 J/cm.

concentration *vs.* radial distance with respect to a linear source for 38 and 150 mW/cm, respectively, for 25, 50, 100 J/cm. Figure 2 (a) shows the sensitizer decreases along with the increase of light fluence, due to photobleaching. The stronger photobleaching is observed in low fluence rate 38 mW/cm (Fig. 2(A)). This phenomena is consistent with low fluence rate inducing higher amount of $^1O_2$ oxygen (Fig. 2(C)), and increasing the reaction probability between $^1O_2$ and ground state photosensitizer. This photobleaching phenomena can also be seen in Fig. 2 (B) as well; that is the stronger photosensitizer degradation inducing faster oxygen recovery for a given fluence. Clearly, the flat regions are observed in these simulated singlet oxygen profiles (Fig. 2(C)), and these plateaus can be possibly related to the PDT induced necrosis distance *in vivo*. We use Fig. 2(C) as the simulated singlet oxygen profiles to test our fitting algorithm to examine the algorithm ability of recovering the critical parameters.

3.2 Demonstration of the fitting algorithm

The robustness of our fitting algorithm is demonstrated in Fig. 3. First, we test 3 photochemical parameters, ξ, ρ, and β, fitting scheme. This scenario is applied to the case g oxygen supply rate known from experiment. We use Fig. 2 (C) 38 – 150 mW/cm, and 25 – 100 J/cm as our simulated data set. The solver we used is the FGRMS iterative solver for our time-dependent system. We tested this solver and it's convergence speed is faster than the other solvers. Fig. 3 (A) shows the fitting results; the

Table 2. Summary of the fitting results for 3 (ξ, ρ, β) and 4 parameter (g,ξ, ρ, β) fits

Fitting scenario	**# of treatment condition, fluence rate and fluence**	**True g:** 0.7	**True ξ:** 3.7×10^{-3}
3 parameters fits	6 (38 and 150 mW/cm, 25 – 100 J/cm)	**Fitted g:** NA	Fitted **ξ:** 3.2×10^{-3}
4 parameters fits	8 (10 and 150 mW/cm, 5 – 100 J/cm	**Fitted ξ:** 0.69	Fitted **ξ:** 3.7×10^{-3}

Fitting scenario	**True ρ:** 7.6×10^{-5}	**True β:** 11.9	**Overall maximum fitting error**
3 parameters fits	**Fitted ρ:** 7.65×10^{-5}	**Fitted β:** 9.0	1.6 %
4 parameters fits	**Fitted ρ:** 7.57×10^{-5}	**Fitted β:** 12.1	0.7 %

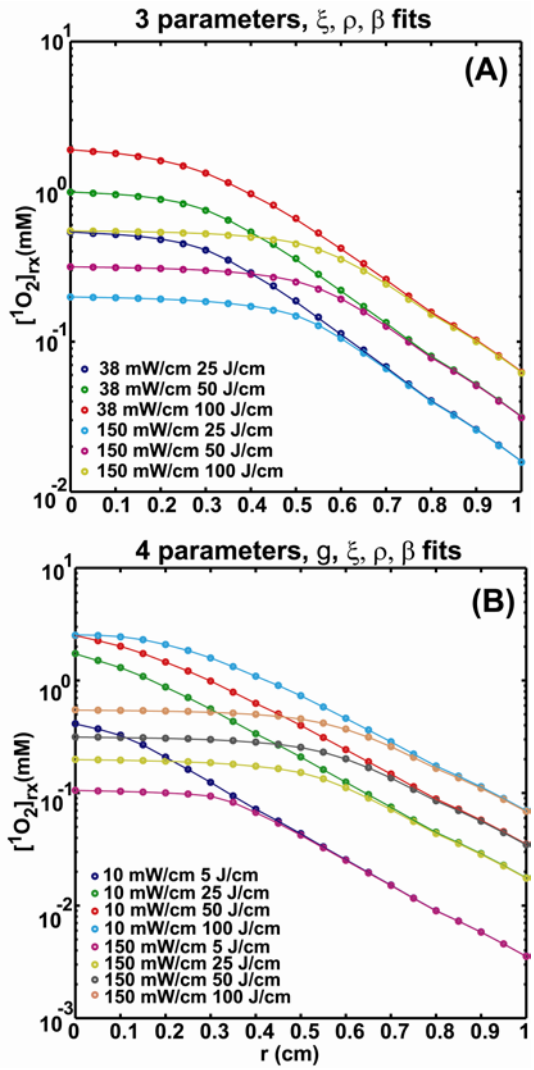

Figure 3: (A) the fit (solid lines) corresponding to the data (symbols) of each case using three photochemical parameters ξ, ρ, β as the fitting parameters; (B) The fit and data using four photochemical parameters g, ξ, ρ and β as the fitting parameters.

symbols are the simulated data, and the solid line are the fits corresponding to each case. The overall maximum fitting error is only 1.6 %, and our algorithm recovers these 3 parameters pretty well. The detail is also specified in Table 2.

Next, we examine our algorithm if it can recover all the 4 parameters; 3 photochemical parameters and 1 physiological parameters, g. Unfortunately, we notice that if we use the same treatment condition (38 – 150 mW/cm and 25 – 100 J/cm Fig. 2(C)), our differential algorithm was not able to recover g and β correctly. The most possible reason is that even for 38 and 150 mW/cm treatment scenario, the $[^1O_2]_{rx}$ profiles are still not distinguishable for 4 parameters fitting. Therefore, we lower the fluence rate down to 10 mW/cm, add additional low fluence cases, 5 J/cm, and then refit the new data set using these 4 parameters. The results are shown in Fig. 3 (B). It is clearly that after introducing the low fluence rate and fluence cases, we are able to get an excellent fit, and recover the 4 parameters well. The overall maximum error is only 0.7 %.

The results in Fig. 3 provide the insight that extreme treatment conditions such as 10 and 150 mW/cm should be considered, to successfully recover the modeling parameters.

A typical computational time for the cases considered in this study is approximately 1 sec for 1 fluence rate running in a desktop computer with Intel Dual Core 2.4 GHz processor and 2 GB of ram. The version of COMSOL is 3.5a and MATLAB is 2007b. Approximately 2500 – 3000 iteration is enough to reach reasonable solutions.

3.3 Preliminary results of interstitial PDT treatment

Preliminary results of a PDT-treated tumor are shown in Fig. 4. An example of our PDT set-up for the interstitial treatment of a shoulder tumor is shown in Fig. 4 (A). Laser light is delivered through a linear diffuser fiber, which is inserted into the catheter through the center of the tumor on an anesthetized mouse, and an isotropic detector is placed at the tumor periphery to monitor treatment light. Figure 4 (B) shows the H&E staining of the tumor treated interstitially with Photofrin-PDT at 150 mW/cm and 25 J/cm. The necrosis region (green highlighted area) is developed surrounding the fiber insertion location (the empty space around the center of the slice). From Fig. 4(B), it is clearly that the developed necrosis region is not a perfect round area. In order to extract a reasonable necrosis region for the fitting purpose, we assumed the total necrosis area equal to a circle area, $r^2\pi$, where r is the calculated necrosis distance we will use for the fitting purpose. For each tumor, we have 8 to 10 slices for calculating the average necrosis. Fig. 3 (C) shows the summary results of the average necrosis distance for 75 and 150 mW/cm treatments ranging from 25 – 100 J/cm. Each

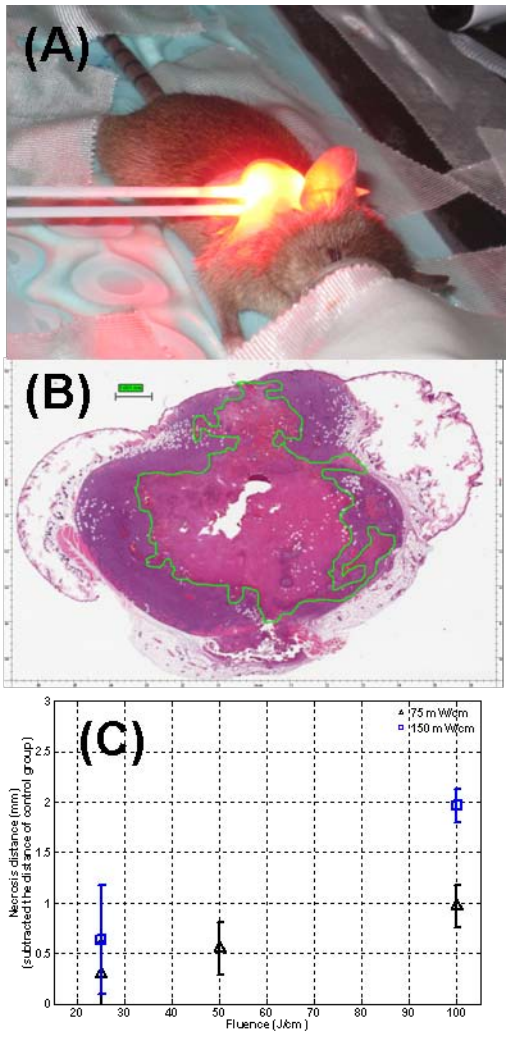

Figure 4. (A) shows a standard interstitial PDT treatment for a shoulder tumor model. (B) shows the H&E staining slice of the tumor treated with Photofrin PDT 150 mW/cm 25 cm, and the necrosis region is circled by green line. (C) summarizes the necrosis distance for 75 and 150 mW/cm treatment *vs.* fluence (J/cm).

symbol represents an average necrosis distance with standard deviation for one mouse. The necrosis effect purely induced by inserting catheter without PDT treatment has been eliminated in these representative distances. As we expected, the PDT-induced necrosis increases along with the fluence for each fluence rate. However, we observe larger necrosis distance at 150 mW/cm than at 75 mW/cm for 100 J/cm (Fig. 4(C)). Due to the merit of low fluence rate treatment, we have longer treatment time and lower oxygen consumption rate than high fluence rate treatment for a given fluence. In the other word, low fluence rate treatment is able to allow larger amount of oxygen replenish the tumor and therefore induce the higher singlet oxygen deposition. This phenomenon is clearly seen in Fig. 2 (B and C). The inconsistency of the necrosis distance observed in Fig. 4(C) for 75 and 150 mW/cm at 100 J/cm is most likely due to the *in vivo* drug concentration uncertainty. We use fluorescence measurement to examine the *in vivo* Photofrin concentration. We found even for the same injection concentration 5 mg/kg, the accumulated drug concentrations within tumor are 7 and 4.3 mg/kg for the case of 150 and 75 mW/cm, respectively.

3.4 Discussion of fitting *in vivo* necrosis distance

The difference between the measured necrosis distance and the singlet oxygen profile is the uncertainty of singlet oxygen threshold dose in an *in vivo* environment. The threshold dose is the dose sufficiently inducing direct tumor cell death, such as necrosis. If the dose is below the threshold dose, there will be no treatment effect [8, 9]. The threshold dose depends on the drug and tumor cell type. So far, there is no data indicating the threshold dose for Photofrin and RIF tumor considered in this study.

To fit the *in vivo* necrosis distance, we can treat the threshold dose as the 5th fitting parameter. An additional experiment of low fluence treatment should be considered. The purpose of this experiment is to find the situation that no PDT-induced necrosis and therefore, we can determine the threshold dose by judging the extension of the plateau.

4. Conclusions

In this work, a COMSOL based singlet oxygen model especially developed for photodynamic therapy is shown. With the appropriate simplification of the model and the calculation power of COMSOL, we are able to solve this model in the scale of one second depending on the number of treatment conditions considered. The corresponding fitting algorithm for necrosis distance is also developed in this work. Using the simulated singlet oxygen profiles, the algorithm is able to recover the

modeling parameters within appropriate accuracy. The future work in our group is to extend the current algorithm by including the extra parameter, threshold dose, and therefore, we are able to fit the *in vivo* necrosis distance and extract the modeling parameters.

5. Acknowledgements

The authors would like to thank Dr. Theresa Busch, Dr. Jarod Finlay, and Mandy Mass for helping with animal experiments. This work is supported by grants from National Institute of Health (NIH) R01 CA 109456 and P01 CA 87971.

6. References

1. S. B. Brown, E. A. Brown, and I. Walker, "The present and future role of photodynamic therapy in cancer treatment," Lancet Oncol. **5**, 497-508 (2004).
2. K.-H. K. Wang, M. T. Busch, J. C. Finlay, and T. C. Zhu, "Optimization of physiological parameter for macroscopic modeling of reacted singlet oxygen concentration in an *in-vivo* model," Proc. of SPIE **7164**, 71640O (2009).
3. T. C. Zhu and X. Zhou, "Finite-element modeling of singlet oxygen during photodynamic therapy," Proc. COMSOL Multiphysics, 189-195 (2007).
4. S. Mitra, and T. H. Foster, "Photophysical parameters, photosensitizer retention and tissue optical properties completely account for the higher photodynamic efficacy of meso-tetra-hydroxyphenyl-chlorin vs Photofrin," Photochem. Photobiol. **81**, 849-859 (2005).
5. T. C. Zhu, J. C. Finlay, X. Zhou, and J. Li, "Macroscopic modeling of the singlet oxygen prodution during PDT," Proc. SPIE **6427**, 642708 642701-642712 (2007).
6. R. Storn and K. Price, "Differential evolution-A simple and efficient heuristic for global optimization over continuous spaces," J. Global Optimization **11**, 341-359 (1996).
7. A. Dimofte, J. C. Finlay, and T. C. Zhu, "A method for determination of the absorption and scattering properties interstitially in turbid media," Phys. Med. Biol. **50**, 2291-2311 (2005).
8. I. Georgakoudi, M. G. Nichols, and T. H. Foster, "The mechanism of Photofrin photobleaching and its consequences for photodynamic dosimetry," Photochem. Photobiol. **65**, 135-144 (1997).
9. T. J. Farrell, B. C. Wilson, M. S. Patterson, and R. Chow, "The dependence of photodynamic threshold dose on treatment parameters in normal rat liver in vivo," Proc. SPIE **1426**, 146 (1991).